

AIAA 79-0465R

# Wind-Tunnel Measurements of Dynamic Reefing Line Force in Ribbon Parachutes

D. F. Wolf\* and R. H. Croll†  
*Sandia Laboratories, Albuquerque, N. Mex.*

This paper presents the results of a series of wind-tunnel tests conducted to measure the force in ribbon parachute reefing lines. Three-foot diameter ribbon parachute models with porosities of 10-25% were tested in the Vought Systems Low-Speed Wind Tunnel. Simultaneous measurement of parachute axial force and reefing line force allowed the latter to be expressed either as a percent of axial force or as a dimensionless force coefficient. Maximum reefing line forces for 15, 20, and 25% porosity chutes were 4-5% of the axial force. Forces for the 10% porosity chute were considerably higher. The 10% porosity chute also showed a significant dynamic effect, with maximum values considerably higher than those in steady state.

## Nomenclature

$C_D$	= drag coefficient $= F_a/qS$
$C_{D1}$	= full open drag coefficient for $L_s = D_c$
$C_{Dr}$	= reefed drag coefficient
$C_l$	= reefing line force coefficient $= T_r/qS$
$D_c$	= parachute constructed diameter = 36 in.
$F_a$	= axial force or drag, lb
$L_r$	= reefing line length, in.
$L_s$	= suspension line length, in.
$q$	= dynamic pressure = 50 lb/ft <sup>2</sup>
$S$	= reference area $= \pi D_c^2/4$
$T_r$	= reefing line force, lb
$\lambda g$	= parachute geometric porosity

## Introduction

THE most widely used method of controlling parachute inflation times and forces is that of reefing, or limiting the radial movement of the parachute skirt with a circumferential line. By cutting the line after a prescribed time delay during which the payload has slowed, the parachute resumes inflating but is subjected to a much reduced inflation force. Multiple reefed stages are often used on systems like Apollo<sup>1</sup> or SRB<sup>2</sup> where weight and volume are at a premium or where forces imposed on the payload must be limited. Common practice has frequently been to overdesign reefing lines because the resulting impact on total parachute weight is small. However, for parachutes with very large design loads this is not possible because the needed materials are either not available or are unwieldy. The price paid for a reefing line failure, on the other hand, is considerable.<sup>3</sup> A reefing line failure usually leads to an immediate or progressive catastrophic failure caused by overloading of the parachute structure. The results of using the CANO<sup>4</sup> stress analysis program to analyze the failure discussed in Ref. 3 were less than satisfying. Predicted reefing line forces from CANO were very sensitive to small pressure differences near the parachute skirt, where it is difficult to measure steady pressures, accurately, let alone unsteady pressures. Because Sandia is frequently required to design ribbon parachutes with large design loads, wind-tunnel tests<sup>5,6</sup> to make direct

measurements of reefing line force were conducted. Nearly all of the data reported herein were taken in the first test,<sup>5</sup> with only a few runs with a Kevlar reefing line included in the later test.<sup>6</sup>

## Model Parachutes

The symmetric, 24-gore, ribbon-type parachutes had a 36 in. nominal diameter across the base of the 20 deg conical construction cone. The suspension line lengths were varied between 1.0, 1.5, and 2.0 times the canopy constructed diameter. The models were constructed of flexible nylon material, with geometric porosities of 10, 15, 20, and 25%. Reefing rings were sewn to the canopy skirt band at each intersection with the 24 suspension lines. A more detailed description of the parachute material, construction technique, and dimensional data has been presented by Pepper and Reed<sup>7</sup> and McVey et al.<sup>8</sup>

## Test Facility

This test series was conducted in the Vought Corporation Low-Speed Wind Tunnel.<sup>9</sup> This tunnel is a horizontal, single-return, closed-circuit facility having tandem test sections of 15 × 20 and 7 × 10 ft in cross section. All of the data presented in this paper were obtained in the 7 × 10 ft test section operating at a dynamic pressure of 50 lb/ft<sup>2</sup>.

The parachutes for this test program were attached to a cable-mounted forebody suspended at the tunnel centerline as shown in Fig. 1. The forebody was a 3.25 in. diameter by 30 in. long ogive cylinder with an ogive radius of 5.69 in. Each parachute was attached to a 2.625 in. diameter ring mounted on a gimbaled drag balance located within the forebody base.

## Test Procedure

The following test technique was utilized to investigate the dynamics of inflation and reefing line forces for symmetric ribbon parachutes. A gimbaled, 500 lb capacity load cell attached to the aft end of the cable-supported forebody measured the parachute total drag or axial force. The reefing line force was measured with a miniature tensiometer located in the reefing line. All data were recorded simultaneously on analog magnetic tape for post-test analysis and on an oscillograph for monitoring purposes. High-speed motion picture coverage (400 frames/s) of the disreefing event were obtained from the two orthogonal views of Figs. 1 and 2 for subsequent more detailed analysis.

A data run consisted of rigging a parachute of selected porosity and suspension line length with the instrumented reefing line of predetermined length between 19 and 67 in.

Presented as Paper 79-0465 at the AIAA 6th Aerodynamic Decelerator and Balloon Technology Conference, Houston, Texas, March 5-7, 1979; submitted May 1, 1979; revision received April 8, 1980. Copyright © 1979 by D.F. Wolf and R.H. Croll. Published by the American Institute of Aeronautics and Astronautics with permission.

\*Member of Technical Staff, Aerodynamics Dept. Associate Fellow AIAA.

†Member of Technical Staff, Aerodynamics Dept.

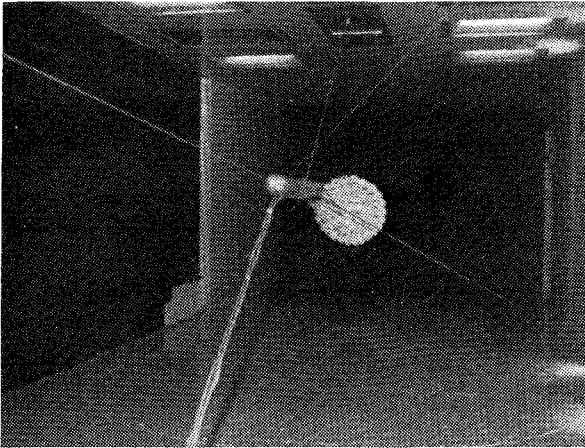


Fig. 1 Test setup—downstream view.

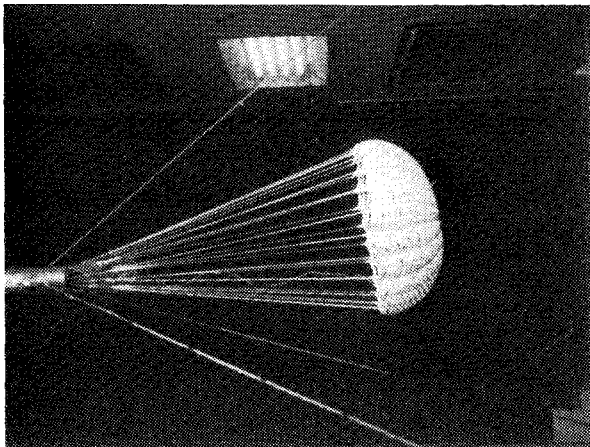


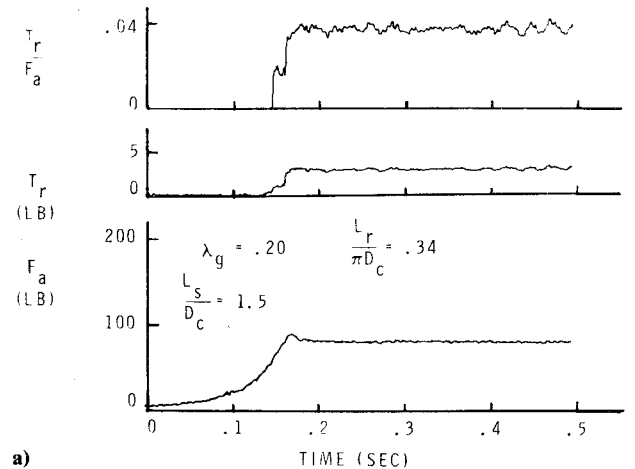
Fig. 2 Test setup—side view.

Next, a 9 in. long reefing line with an electrically initiated line cutter on it was installed through the same reefing rings. Care was taken to separate the pyrotechnic line cutter from the reefing line tensiometer, the knots, and the reefing rings in order to promote an unobstructed smooth disreefing. The reefing line tensiometer<sup>‡</sup> was a small strain-gaged hollow cylindrical tube which had been bonded on the reefing line cord. The tube was 0.6 in. long with a 0.09 in. outside diameter.

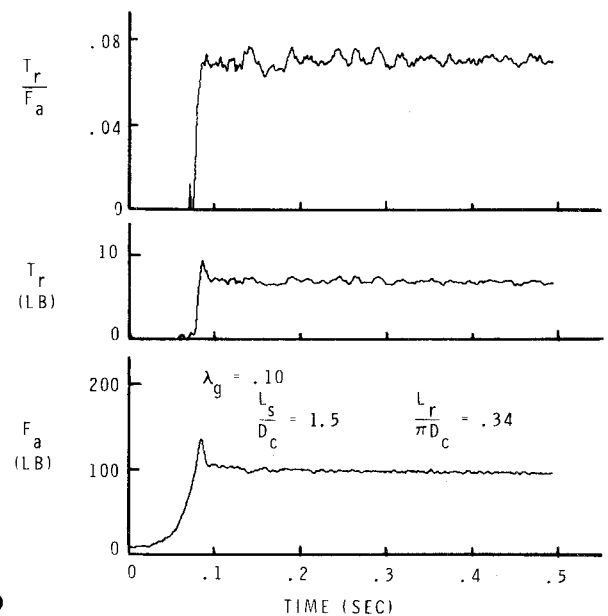
After tunnel flow was stabilized at the desired dynamic pressure, a sequence timer was activated to start the high-speed motion picture cameras, trigger the event marker, and fire the cutter on the 9 in. reefing line. The analog magnetic tape recorder and oscillograph were manually started before initiation of the sequence timer. The event marker consisted of firing a flash bulb for the movie cameras and providing a voltage step on the tape recorder which occurred coincident with cutting the 9 in. reefing line. The parachute then inflated from its fully reefed condition (9 in. line) to its next reefed (instrumented) condition. Data were taken continuously from 5 s before the event until 1 s after the inflation was initiated.

### Data Reduction

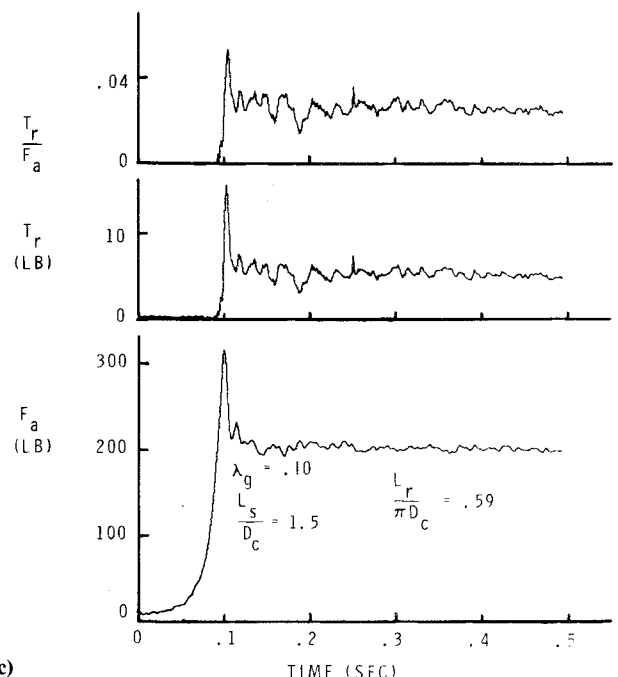
Reduced data plots and tabular listings were obtained by digitizing the analog magnetic tapes at Sandia after the test. The tapes were played into the Sandia Data Acquisition and Control System<sup>10</sup> and digitized at the rate of 1000 samples/s. Typical digital plots of the disreefing event are shown in Fig.



a)



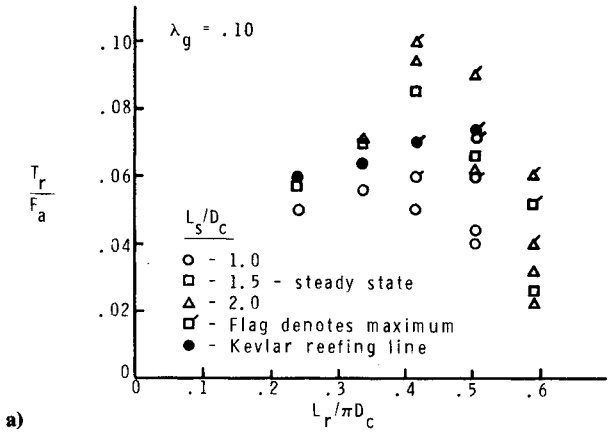
b)



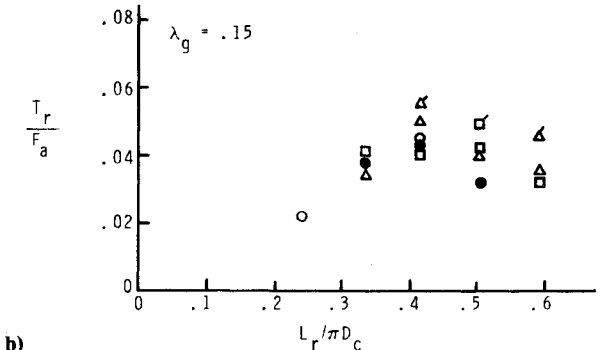
c)

Fig. 3 Sample digital data plot.

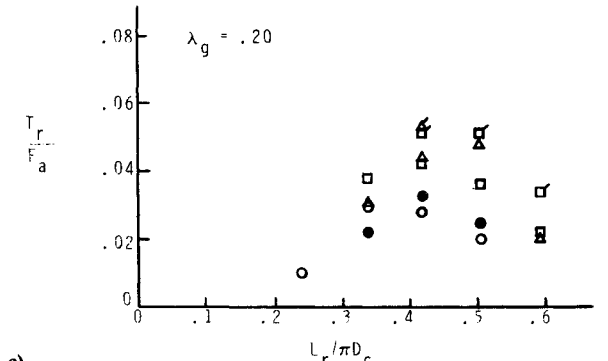
<sup>‡</sup>Cord load transducers manufactured by Precision Measurements Co., Ann Arbor, Mich.



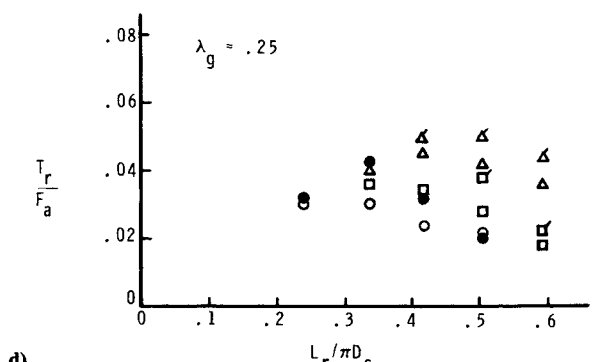
a)



b)

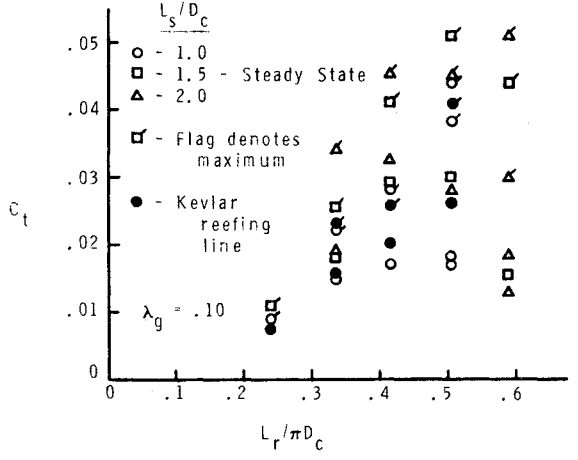


c)

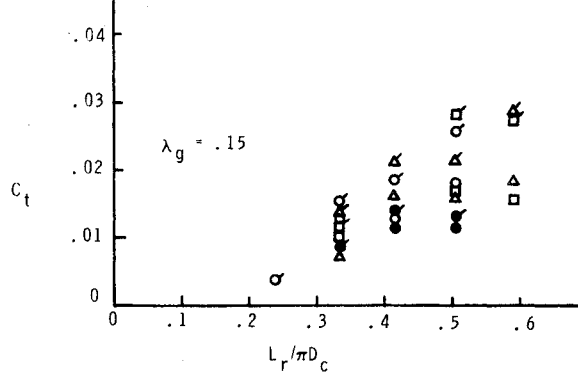


d)

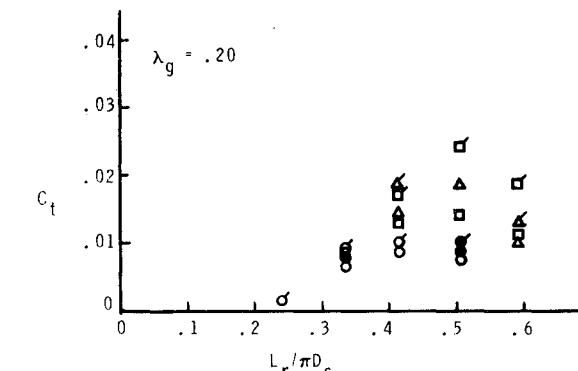
Fig. 4 Ratios of reefing line force to axial force.



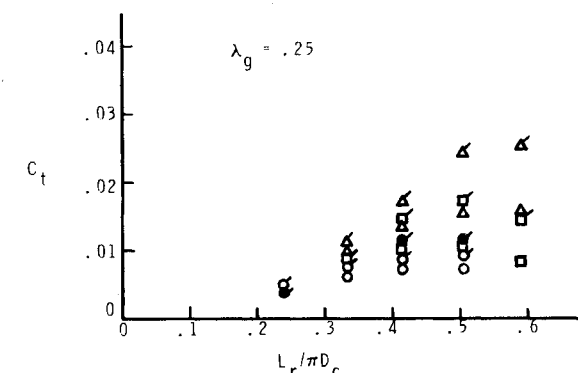
a)



b)



c)



d)

Fig. 5 Reefing line force coefficients.

3. As a part of the data reduction, the ratio of reefing line force to axial force was also formed and plotted as shown in Fig. 3.

Even though considerable care was taken in rigging the instrumented reefing line, the tensiometer occasionally would "hang up" on a reefing ring during inflation. The strain gage could measure something other than pure tension when this happened, causing erroneous results. It is possible that some

data containing errors of this type are included in this paper, particularly for the reefing line force transient. All runs where the tensiometer obviously "hung up" were either repeated or the data are not presented.

Data Analysis

The conventional way of analyzing reefing line force data is to look at the ratio of reefing line force to axial force. A static

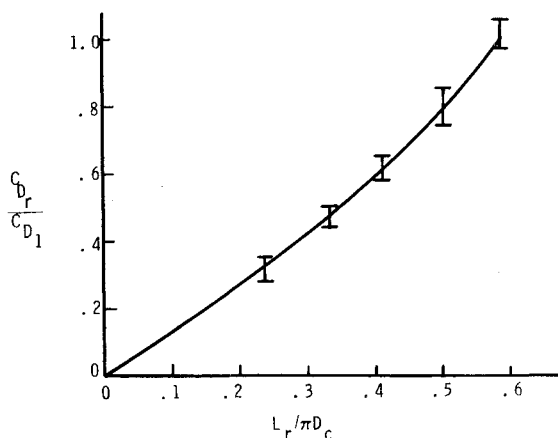


Fig. 6 Ratios of reefed drag coefficient to full open drag coefficient with  $L_s = D_c$ .

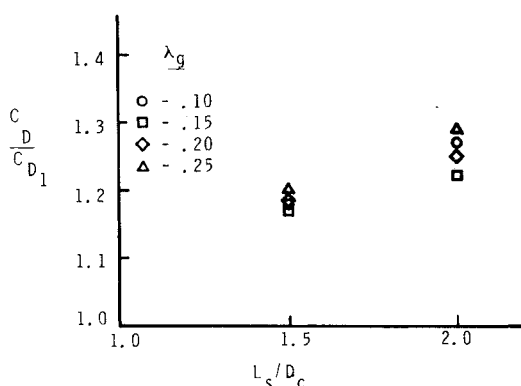


Fig. 7 Drag coefficients for longer suspension lines.

force balance at the parachute skirt<sup>11</sup> suggests that this is the proper way to normalize reefing line forces. From plots such as those in Fig. 3 the maximum and steady-state values for the ratio were read for all wind tunnel runs. The results are plotted in Fig. 4 for the four different porosity chutes tested as a function of reefing line length. The three higher porosity chutes all show upper limit steady-state ratios in the 4-5% range. This is consistent with design criteria used for reefing lines of modern ribbon parachutes.<sup>1,2</sup>

The 10% porosity chute showed considerably higher steady reefing line forces of about 6% of the measured axial force. This is not surprising in view of the larger inflation forces generated by low-porosity chutes. The effect of suspension line length is also shown. Longer suspension lines result in larger reefing line forces as expected, particularly for the longer reefing line lengths. As explained in Ref. 11, reefing line force is proportional to the angle between the suspension lines and radials at the parachute skirt. This angle increases with increasing suspension line length for a reefed parachute.

Also shown in Fig. 4 are some dynamic peak values taken from plots of reefing line force/axial force ratios. Because the ratio was derived from a static force balance, it is not as useful in interpreting the dynamic data. The dynamic peaks in the ratio are not as repeatable as the steady-state values. An inflating parachute is a complex, multiple degree-of-freedom system, so the reefing line force transient and axial force transient do not always remain in phase for small changes in initial conditions or test parameters. It was often not clear whether the ratio peaked because the reefing line force had peaked, or the axial force had peaked earlier and had already decreased. Because of the uncertainties in how to interpret the dynamic peak values of reefing line force/axial force ratio, it

is difficult to give a simple recommendation about how to use the data for design. The situation becomes even more confused for a finite-mass system where significant deceleration occurs between the time peak axial force occurs and the time peak reefing line force occurs. For finite-mass systems the axial force at the time of peak reefing line force should be used. That information may be difficult to obtain for large parachutes used on small payloads.

For the reasons given above, an alternate method of analyzing the reefing line force data was explored. Dynamic and steady-state values of reefing line force were reduced to a dimensionless coefficient form by dividing the force by the product of dynamic pressure times a reference area. This, of course, is the conventional method of scaling aerodynamic force data to different sized bodies and different test conditions. The results are shown in Fig. 5 for the four different porosity parachutes over the range of reefing line lengths tested. A few observations are made regarding these data. First, the ratio of dynamic peak to steady-state value of the force coefficient is much larger for the 10% porosity chute than for the other three chutes. This should not be surprising when the more violent nature of low-porosity parachute inflations is considered. Also, the ratio of dynamic peak to steady-state force coefficient is very large for the longer reefing lines tested. The longer reefing lines serve primarily as overinflation control lines, taking a high dynamic force to prevent overinflation but a much reduced force when the parachute assumes its steady-state configuration. No significant difference between data taken with nylon and Kevlar reefing lines was observed. This was partly due to the range of reefing line forces and reefing line strengths, however. Both materials were relatively stiff, because forces of about 10 lb were being taken by a 100 lb nylon line and a 400 lb Kevlar line. The stiffness effect should be explored in more detail for lines that are heavily loaded.

Reefing line force data are often presented as a function of drag area ratio (ratio of reefed drag coefficient to full open drag coefficient) rather than the line length ratio used in Figs. 4 and 5. The reader can convert on an approximate basis to the drag area ratio form using Figs. 6 and 7. Figure 6 shows the ratio of reefed drag coefficient for all suspension line lengths to full open drag coefficient for a suspension line length of one constructed diameter. All parachutes tested fall within the fairly narrow scatter band shown, indicating the expected result that reefed drag coefficient is not a strong function of suspension line length. Figure 7 presents full open drag coefficient data for longer suspension line lengths. With Figs. 6 and 7 a reefed drag area ratio for an arbitrary reefing line length and suspension line length can be calculated approximately for the parachutes tested.

## Conclusions

Steady reefing line forces of 4-5% of the parachute axial force were measured on ribbon parachute models of 15, 20, and 25% geometric porosity. Higher reefing line forces were measured on a 10% porosity chute. Dynamic reefing line forces remained large for long reefing lines (near full open parachutes) even though steady reefing line forces decreased for these configurations. An alternate reefing line force coefficient form of analyzing the data makes it somewhat easier to interpret the dynamic force data.

## Acknowledgments

The work reported here was supported by the U.S. Department of Energy. Appreciation is given to the following Sandia personnel for assisting with this project: D. R. MacKenzie and D.A. Powers for providing instrumentation and data reduction; K.L. Ronquillo and H.E. Widdows for parachute rigging; J.T. Cowie for high-speed motion picture coverage; and from Vought Corporation, Grand Prairie, Texas, J. W. Holbrook and R. H. Oldenbuttel for conducting the wind-tunnel tests.

## References

- <sup>1</sup>Knacke, T.W., "The Apollo Parachute Landing System," Paper presented at AIAA 2nd Aerodynamic Decelerator Systems Conference, El Centro, Calif., Sept. 1968.
- <sup>2</sup>Mitchell, R.A., "Space Shuttle Solid Rocket Booster Recovery System," *AIAA 6th Aerodynamic Decelerator and Balloon Technology Conference Proceedings*, Houston, Texas, March 1979.
- <sup>3</sup>Runkle, R.E., "Space Shuttle Solid Rocket Booster Decelerator Subsystem Drop Test 3 - Anatomy of a Failure," Paper 79-0431, *AIAA 6th Aerodynamic Decelerator and Balloon Technology Conference Proceedings*, Houston, Texas, March 1979.
- <sup>4</sup>Reynolds, D.T. and Mullins, W.M., "Stress Analysis of Ribbon Parachutes," Paper 75-1372 presented at AIAA 5th Aerodynamic Deceleration Systems Conference, Albuquerque, N. Mex., Nov. 1975.
- <sup>5</sup>Holbrook, J.W., "A Low Speed Wind Tunnel Test of Parachute Reefing Line Loads and Symmetric Inflation Techniques," Vought Systems Division, Dallas, Texas, LSWT-560, May 29, 1978.
- <sup>6</sup>Holbrook, J.W., "A Low Speed Wind Tunnel Test of Sandia Laboratories Modified Modular Lifting and Lift-to-Airburst Parachutes," Vought Systems Division, Dallas, Texas, LSWT-573, Nov. 1978.
- <sup>7</sup>Pepper, W.B. and Reed, J.F., "Parametric Study of Parachute Pressure Distribution by Wind Tunnel Testing," *Journal of Aircraft*, Vol. 10, Nov. 1976, pp. 895-900.
- <sup>8</sup>McVey, D.F., Pepper, W.B., and Reed, J.F., "A Wind Tunnel Parametric Study of Ribbon Parachutes," Paper 75-1370 presented at AIAA 5th Aerodynamic Deceleration Systems Conference, Albuquerque, N. Mex., Nov. 1975.
- <sup>9</sup>Holbrook, J.W., "Low Speed Wind Tunnel Handbook," Vought Corporation, Publication AER-EOR-12995-B, July 1978.
- <sup>10</sup>Croll, R.H. and Forsythe, F.E., "A Computer-Controlled Data Acquisition and Control System for Wind Tunnel Testing," Sandia Laboratories, Albuquerque, N. Mex., SC-DC-68-2528, Dec. 1968.
- <sup>11</sup>Ewing, E.G., "Ringsail Parachute Design," Technical Report AFFDL-TR-72-3, Wright-Patterson Air Force Base, Ohio, Jan. 1972.

*From the AIAA Progress in Astronautics and Aeronautics Series...*

## ENTRY HEATING AND THERMAL PROTECTION—v. 69

## HEAT TRANSFER, THERMAL CONTROL, AND HEAT PIPES—v. 70

*Edited by Walter B. Olstad, NASA Headquarters*

The era of space exploration and utilization that we are witnessing today could not have become reality without a host of evolutionary and even revolutionary advances in many technical areas. Thermophysics is certainly no exception. In fact, the interdisciplinary field of thermophysics plays a significant role in the life cycle of all space missions from launch, through operation in the space environment, to entry into the atmosphere of Earth or one of Earth's planetary neighbors. Thermal control has been and remains a prime design concern for all spacecraft. Although many noteworthy advances in thermal control technology can be cited, such as advanced thermal coatings, louvered space radiators, low-temperature phase-change material packages, heat pipes and thermal diodes, and computational thermal analysis techniques, new and more challenging problems continue to arise. The prospects are for increased, not diminished, demands on the skill and ingenuity of the thermal control engineer and for continued advancement in those fundamental discipline areas upon which he relies. It is hoped that these volumes will be useful references for those working in these fields who may wish to bring themselves up-to-date in the applications to spacecraft and a guide and inspiration to those who, in the future, will be faced with new and, as yet, unknown design challenges.

*Volume 69—361 pp., 6 × 9, illus., \$22.00 Mem., \$37.50 List*  
*Volume 70—393 pp., 6 × 9, illus., \$22.00 Mem., \$37.50 List*

TO ORDER WRITE: Publications Dept., AIAA, 1290 Avenue of the Americas, New York, N.Y. 10104